THE VAPORIZATION OF PYROLYTIC GRAPHITE

SPACE SCIENCES
LABORATORY

SPACE SCIENCES LABORATORY

RE-ENTRY PHYSICS SECTION

THE VAPORIZATION OF PYROLYTIC GRAPHITE*

By

P. D. Zavitsanos

R66SD31
May, 1966

MISSILE AND SPACE DIVISION

GENERAL ⬤ ELECTRIC

CONTENTS

	PAGE

ABSTRACT

The vaporization of surface nucleated pyrolytic graphite was studied using a microbalance-target technique to measure total effusion and vaporization rates, and the time-of-flight mass spectrometer to determine the relative contribution of the three major gaseous species C, C_2 and C_3 under equilibrium and non-equilibrium conditions.

Knudsen effusion measurements were made in the temperature range $2417^\circ K$ - $2700^\circ K$ and vapor pressure values were obtained for C, C_2 and C_3. Respective heats of vaporization, ΔH°_{298}, calculated by the third-law method, with free energy functions from the JANAF Tables, are 173.5 ± 1, 203.5 ± 1.1 and 192 ± 1 kcal·mole^{-1}.

If a bending frequency of 63-70 cm^{-1} is used for C_3 (as recently reported by Gansset et al) the heat of vaporization ΔH°_{298} (as calculated by the third law method) is 207 kcal · mole^{-1}. The latter value is in serious disagreement with the value of 186.7 ± 1.7 kcal·mole^{-1} obtained by Drowart et al from mass spectrometric results and the second-law method.

Using the high value (207) for the heat of vaporization the vapor pressure of C_3 was calculated to $4600^\circ K$.

Langmuir vaporization measurements were carried out in the temperature range $2250^\circ K$ - $2760^\circ K$. The ratios of vaporization coefficients obtained from mass spectroscopic measurements are: $\dfrac{\alpha_2}{\alpha_1} = 2.1$, $\dfrac{\alpha_1}{\alpha_3} = 10.6$. Use of vapor pressure data and vaporization rates was made to arrive at an overall vaporization coefficient equal to 0.095 and individual values of $\alpha_1 = 0.24$, $\alpha_2 = 0.50$ and $\alpha_3 = 0.023$.

I. INTRODUCTION

Graphite has been receiving a great amount of attention as a structural material in aerospace applications. The advantages of this material are:

1. Resistance to sublimation
2. High strength to density ratio at high temperatures
3. Resistance to thermal shock

It has also been known since 1883 that through the pyrolysis of hydrocarbons at high temperatures (1800-2200°C) one can make a form of highly oriented graphite with very high density and extremely low porosity. This material is called pyrolytic graphite and due to its anisotropy possesses interesting properties, such as very low thermal conductivity in the C-direction and high oxidation resistance[1,2] compared to regular graphite.

Since the vaporization behavior of high performance tips and heat shields constitutes an important input to aerodynamic calculations of weight loss, boundary layer chemistry and observables, it is significant to know: (1) gross rate of sublimation, (2) composition of the resulting vapor and partial pressures of the resulting species, (3) vaporization coefficients for the gaseous carbon species so that the composition of the boundary layer can be predicted more accurately for non-equilibrium conditions. Incomplete knowledge of the above properties warranted the following study.

II. EXPERIMENTAL

The specimens of pyrolytic graphite used in these studies were taken
from a surface nucleated piece manufactured by the Metallurgical Products
Department, General Electric Company, Detroit. The material had a density
of 2.21 g. cm^{-3} and high purity. The ash content was about 0.005% by weight.
Spectroscopic analysis of the ash content is shown below:

Si	50%
Al	6
Ca	5
Zr	3
V	2
Fe	3
Ti	0.7
Ta	1
W	1
Ni	0.5
B	0.03
Oxygen	Bal.

A. MICROBALANCE-TARGET TECHNIQUE

1. Knudsen Effusion

The vaporization of pyrolytic graphite was studied by using the Knudsen
effusion target method with a recording microbalance. A conical target, made
of molybdenum sheet (or glass), Figure 1, intercepted a well defined fraction
of the vapor effusing from a Knudsen crucible, Figure 2. The weight increase
of the target due to the condensation of carbon vapor was recorded by a
Sartorius-Electrona microbalance. A sketch of the apparatus is shown in
Figure 3; a detailed description of the apparatus with applications was given
previously[3], [4], [5].

The crucibles used were made of tantalum and tungsten and had
several orifice sizes. In general the orifice to sample-surface ratio was
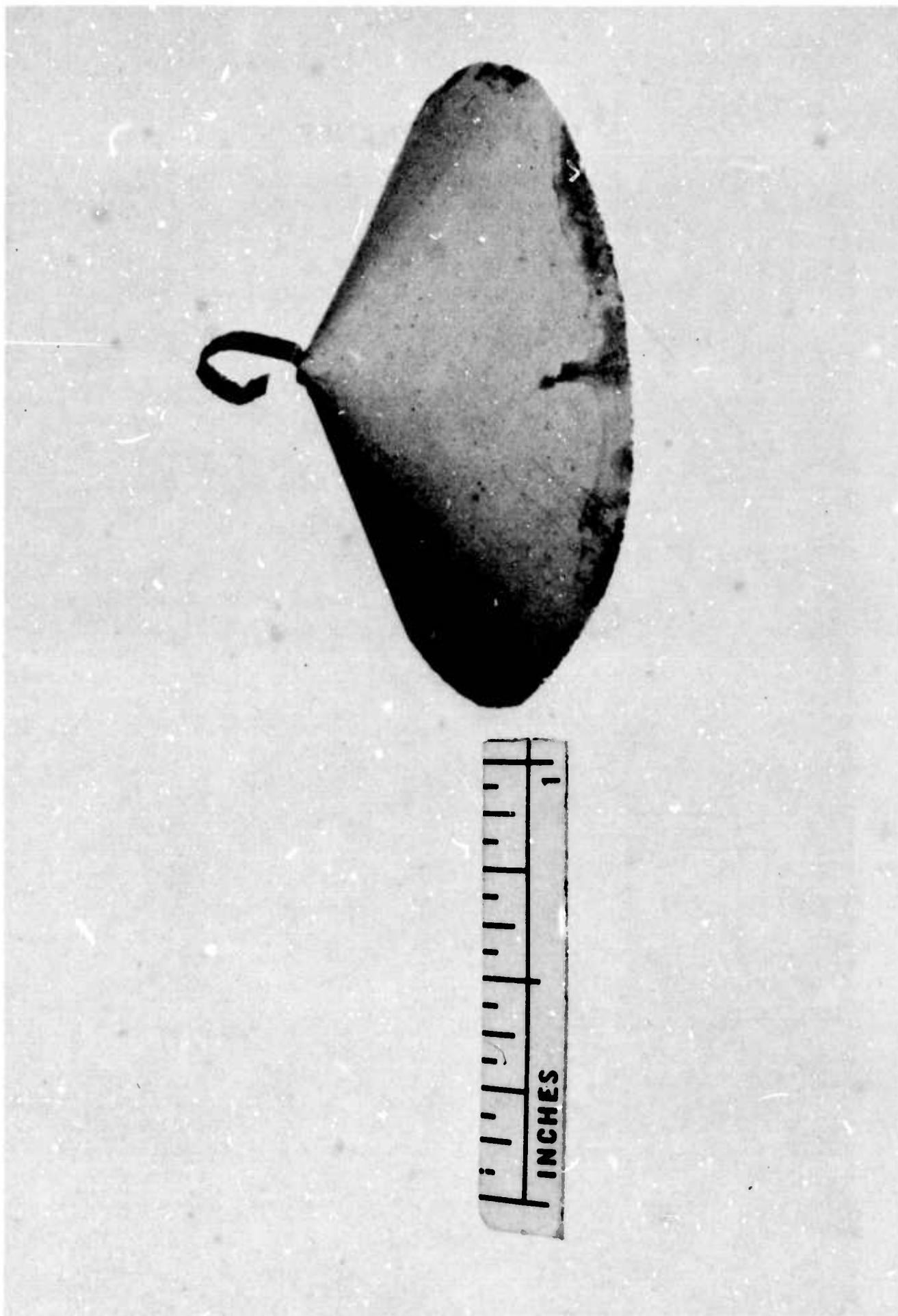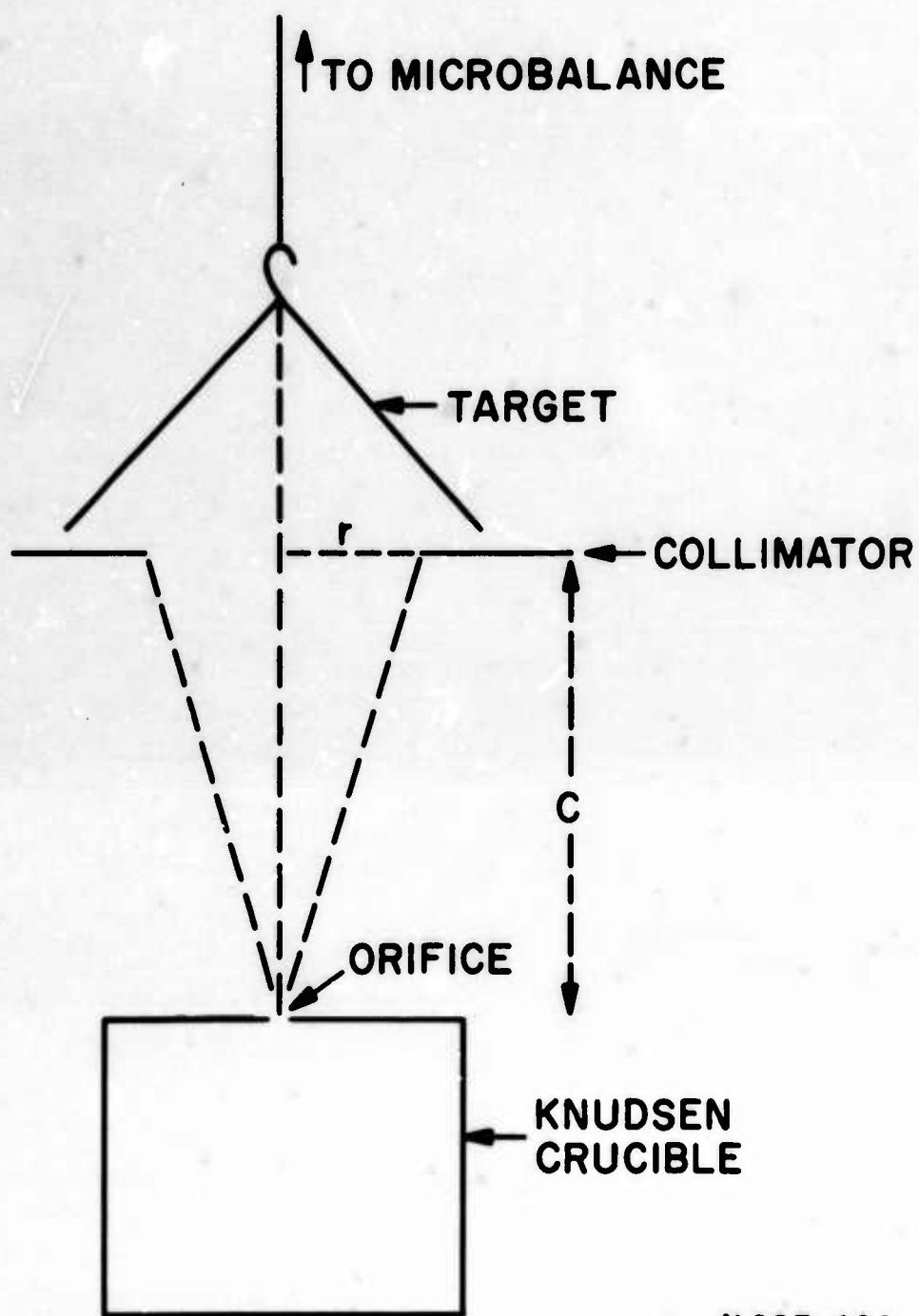always less than 10^{-3}. Electron bombardment was used for heating and the

2

Figure 1. Molybdenum Target

3

TO MICROBALANCE

TARGET

COLLIMATOR

r

C

ORIFICE

KNUDSEN
CRUCIBLE

N 207-409

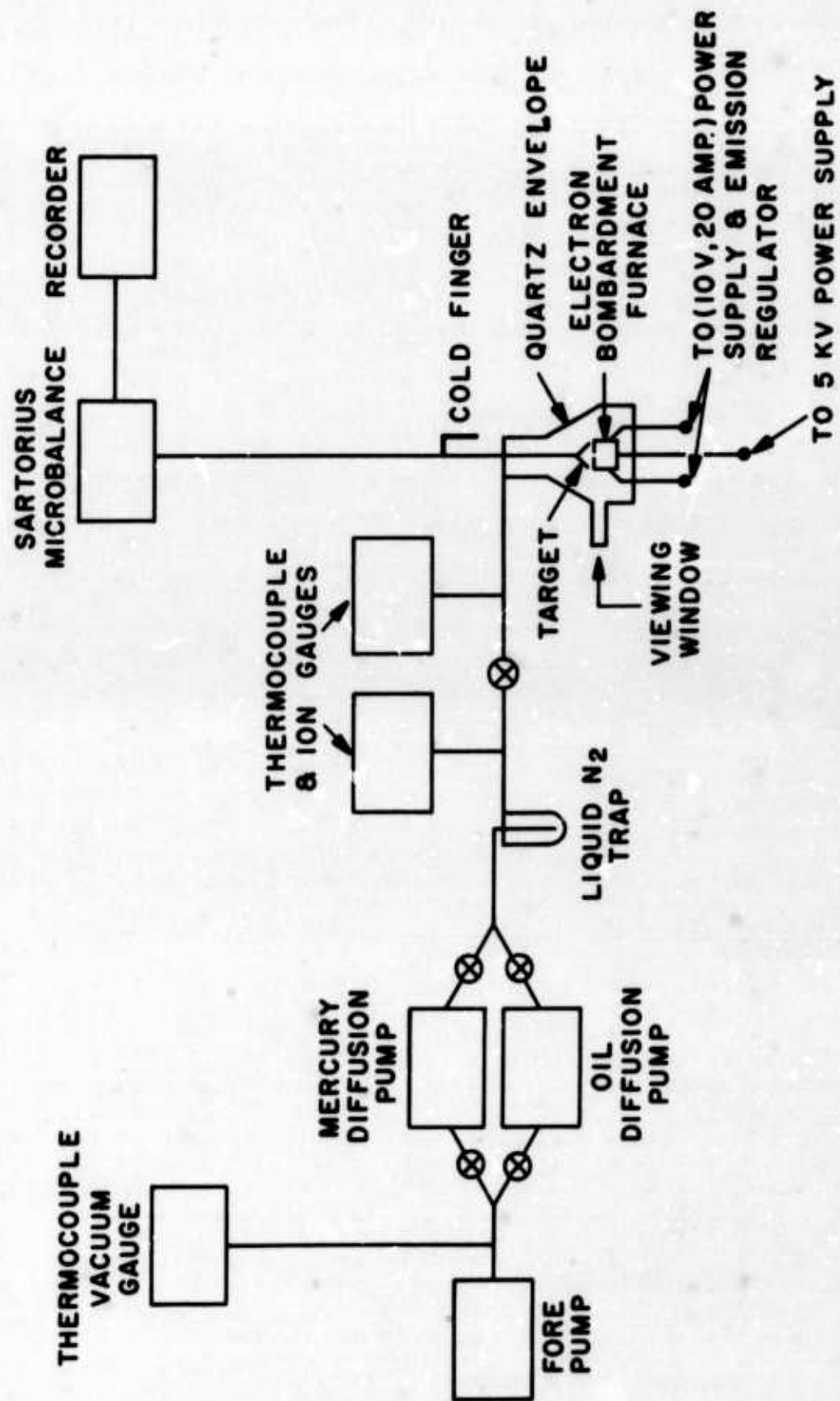Figure 2. Geometry of Knudsen Crucible and Target

Figure 3. Microbalance Apparatus

5

temperature was measured with a calibrated optical pyrometer by sighting into a black-body hole drilled on the side of the crucible. The optical pyrometer was calibrated against an NBS lamp. A quartz window used for sighting was kept clean (from vapors) with an iron slug which (actuated from outside with a small magnet) was removed from the window only during temperature measurements.

2. Langmuir Vaporization

In addition to the effusion measurements rates of sublimation were measured by heating cylinders of pyrolytic graphite in vacuum by electron bombarding. The cylinders (2.5 cm dia. x 1.5 cm long) were mounted in the same manner as the Knudsen crucible in the same apparatus. Temperature measurements were made pyrometrically by sighting into a black body hole drilled on the specimen. Rates of vaporization from the plane perpendicular to the C-axis were obtained with the same microbalance-target technique by measuring the condensation rate of carbon vapor vaporizing from a surface area equal to the hole of the shield, 1.1 cm^2.

B. MASS SPECTROMETRY

Using electron bombardment again for heating and the Bendix Time-of-Flight Mass Spectrometer, the vapor resulting from the vaporization of pyrolytic graphite was analyzed as a function of temperature under conditions of equilibrium and non-equilibrium.

A diagram of the electron bombardment furnace and part of the mass spectrometer is shown in Figure 4. The Knudsen crucible A, kept at positive voltage (0-5 kv) is heated by electron bombardment from a heated tungsten filament B. Temperatures as high as 2500°C were reached with control of ± 2°. Temperature control was achieved by keeping the emission current constant through automatic regulation of the filament current. A circuit diagram of the emission regulator was given elsewhere[4]. In order to prevent furnace ions from entering the mass spectrometer and reduce background noise, negative voltage was applied on shield C (Figure 4). By keeping the absolute value of the biasing negative voltage slightly higher than the

A – CRUCIBLE
B – TUNGSTEN FILAMENT
C – TANTALUM SHIELD
D – SHUTTER-CHAMBER
E – MOVABLE SHUTTER
F – TOF SOURCE ENTRANCE SLIT
G – IONIZING ELECTRON BEAM
H – ION GRID
I – VIEWING WINDOW
J – PRISM
K – OPTICAL PYROMETER

TO MULTIPLIER

FIELD FREE FLIGHT TUBE

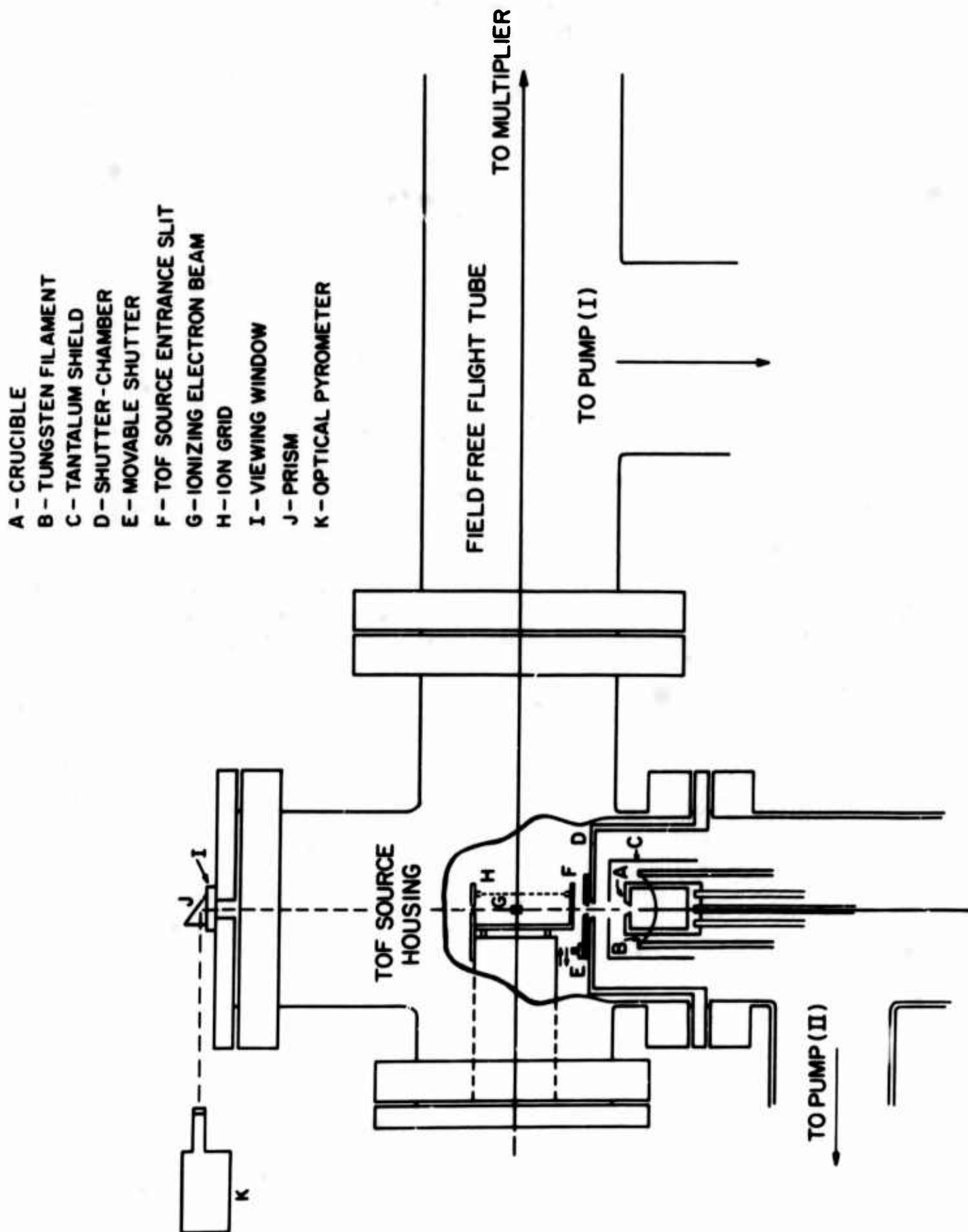TO PUMP (I)

TOF SOURCE HOUSING

TO PUMP (II)

Figure 4.   Electron Bombardment Furnace and Time of Flight Mass Spectrometer

7

positive voltage of the crucible ions with positive charge are either collected or deflected by the shield so that they do not enter the ion source of the mass spectrometer. A grounded crucible-negative filament arrangement was also used. This second heating arrangement appeared to give less background noise and is considered preferable. The temperature was measured in the same manner as previously described with an additional correction for the prism (Figure 4).

After proper collimation a small fraction of the vapor effusing from the cell enters the ionization region of the ion source where a pulsed electron beam (directed perpendicular to the neutral beam) ionizes a fraction of the gas. The resulting positive ions are pulsed by ion grid H (-2.8 kv) and all receive an equal energy impulse. Since their respective velocities vary according to their mass to charge ratios (m/e) the ions are separated in bunches of equal m/e. As each bunch strikes the collector cathode, it is converted into an electron signal and through secondary electron emission in the electron multiplier is amplified. The resultant (amplified) electron pulses pass across a resistor and the resulting voltage pulses (after further amplification in the wide band amplifier) are displayed on an oscilloscope screen and compose the mass spectrum. (The lighter masses appear on the left of the screen). The oscilloscope is triggered by a pulse whose timing relative to that of the ion focus pulse can be varied. Mass spectrometer ion signals can be also obtained by using the analog output. The analog unit integrates many single-sweep spectra which are detected by a gate. A single-sweep spectrum results from one cycle of operation at a rate of 10^4 per second. The gate sweeps the spectrum (at a slowly and linearly increasing time delay with respect to the ionization pulse) and represents the average of a number of ionization pulses at each mass peak. The data reported in this document were obtained by using the analog unit.

A detailed picture of the furnace assembly is shown in Figure 5. In all the effusion experiments tantalum cells were used. Non-equilibrium (Langmuir) vaporization was also carried in the mass spectrometer. This
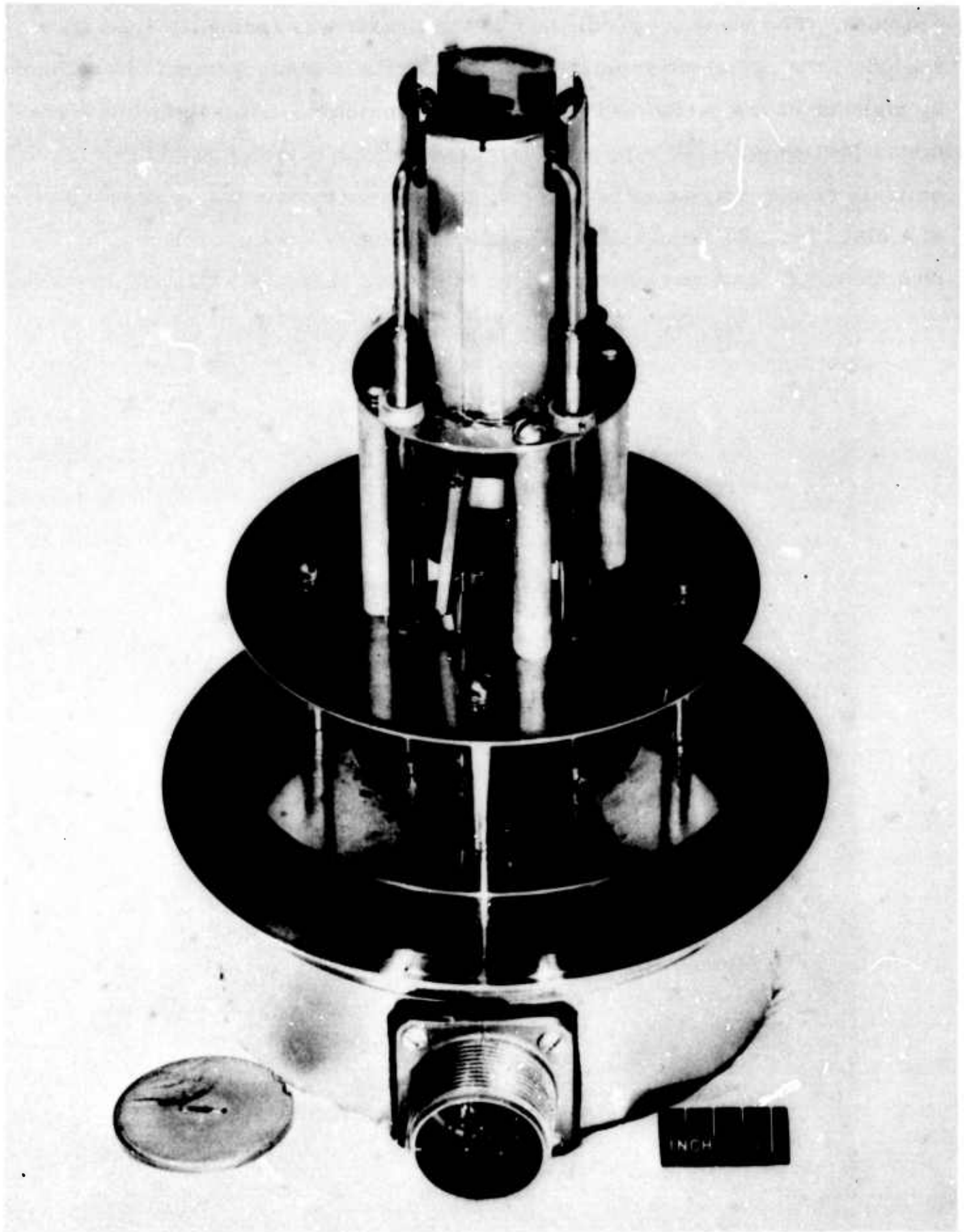
8

Figure 5. Knudsen Crucible Attachment

was done by replacing the crucible with a cylindric specimen of pyrolytic graphite. The plane perpendicular to the C-axis was facing the ionization region of the mass spectrometer and temperature measurements were made by sighting at the surface with an optical pyrometer. Emissivity measurements by DeSantis[5a] were used to correct the pyrometer readings. The emissivity corrections were checked in a separate experiment by looking at a black body hole and the basal plane with the optical pyrometer. A photograph of the mass spectrometer is shown in Figure 6.
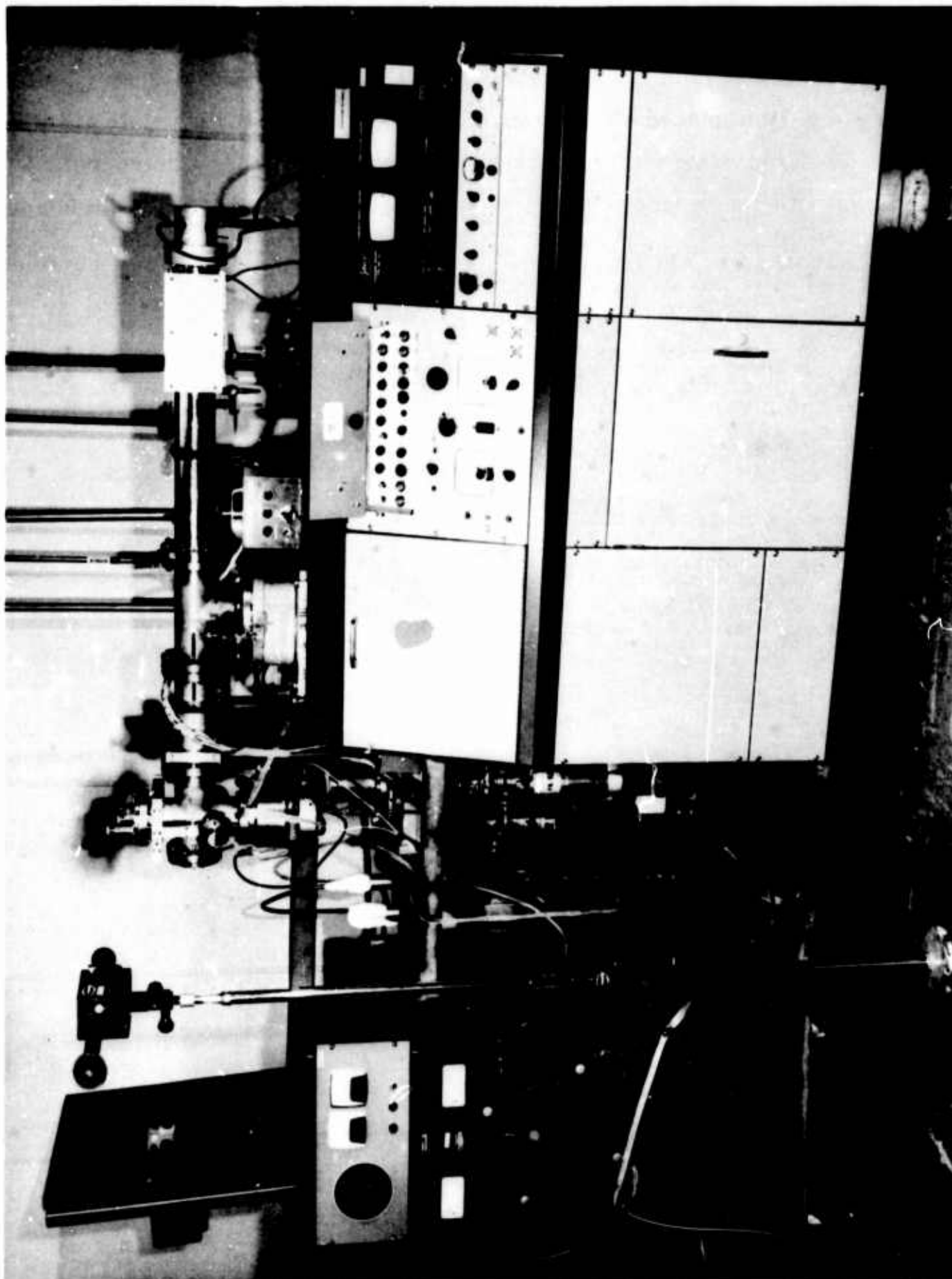
Figure 6. Time of Flight Mass Spectrometer

III. RESULTS

A. KNUDSEN EFFUSION

Knudsen crucibles with three different orifice-sizes (.0109, .0126, 0.0248 cm^2) were used in the microbalance experiments. A collimator with a radius $r = 0.3$ cm placed at a distance $c = 1.5$ cm from the crucible allows a fraction of the effusing vapor to strike the target. Increases in the weight of the target (ΔW) as a function of time (Δt) are shown in Table I. The condensation rate m' (gm. sec^{-1}) is $\frac{10^{-6} \Delta W}{60 \, \Delta t}$; effusion rates m are then obtained from

$$m = m' \left[(c^2 + r^2)/r^2 \right] A^{-1} \tag{1}$$

where A is the area of the orifice. Rates of effusion obtained in the temperature range $2417^\circ K$ - $2700^\circ K$ are shown in Table I. Comparison with the effusion data of Brewer et al[6] taken on spectroscopic grade graphite shows good agreement. The equilibrium vapor pressure, P, is to be calculated from the Knudsen equation

$$P = m (2\pi \, RT/M)^{1/2} \tag{2}$$

where m is the effusion rate in gm. cm^{-2} sec^{-1}, T is the temperature in $^\circ K$, and M is the molecular weight of the vapor. In the case of graphite the vapor consists of atomic as well as molecular species (i.e. C_1, C_2, C_3, C_4, C_5 ...) and in these experiments the total effusion rate is measured, $m = \sum_i m_i$. As shown by previous mass spectrometric work[7], [8] and verified by this investigation, the important species, in the temperature range of this work, are C_1, C_2, and C_3 and therefore

$$m = \left(\frac{12}{2\pi \, RT} \right)^{1/2} \left\{ P_{C_1} + \sqrt{2} \, P_{C_2} + \sqrt{3} \, P_{C_3} \right\} \tag{3}$$

By measuring ratios of ion intensities I_n/I_1, for the species in question by the time-of-flight mass spectrometer, the following expressions can be used:

Table I

VAPORIZATION OF PYROLYTIC GRAPHITE
KNUDSEN-MICROBALANCE TECHNIQUE

Run No.	$T^{\circ}K$	$\Delta W(\mu g)$	$\Delta t(min)$	$\dfrac{c^2 + r^2}{r^2}$	$A \times 10^2 cm^2$	Effusion Rate- $m \times 10^7\ gm\,cm^{-2}\ sec^{-1}$
19-A-1	2564	12	61	22.436	1.095	36.6
19-A-3	2595	34	178	22.436	1.266	56.41
19-A-4	2562	29	180	14.58	1.095	27.873
19-A-5	2518	26	320	14.580	1.266	17.702
20-A-2	2565	38	330	14.580	1.095	25.518
56	2422	10	235	10.269	2.48	2.936
57	2452	25.5	180	10.269	2.48	9.7931
59	2417	25	240	10.269	2.48	7.1716
61	2515	29	120	10.269	2.48	16.62
66	2482	24	330	10.269	2.48	4.231
67	2700	251.8	100	10.269	2.48	173.8

$$\frac{P_{C_2}}{P_{C_1}} = \frac{I_2}{I_1} \times \frac{\sigma_1}{\sigma_2} \times \frac{(E-A_1)}{(E-A_2)} \qquad (4)$$

$$\frac{P_{C_3}}{P_{C_1}} = \frac{I_3}{I_1} \times \frac{\sigma_1}{\sigma_3} \times \frac{(E-A_1)}{(E-A_3)} \qquad (5)$$

where σ = relative cross section for ionization, E = energy of ionizing electrons, A = appearance potential ($A_1 = 11.3$, $A_2 = 12$, $A_3 = 12.6$ volts). All the results were obtained at a low electron energy (i.e. $E = 20$ volts) in order to avoid fragmentation of the molecular species. Additivity of cross sections was assumed[9] i.e.

$$\sigma_1/\sigma_2 = 1/2; \quad \sigma_1/\sigma_3 = 1/3.$$

Mass spectrometric data obtained in the temperature range $2500^\circ K$ - $2755^\circ K$ are shown in Table II.

Vapor pressures obtained from the combination of microbalance and mass spectrometric techniques through equations (3), (4), and (5) are shown in Table III and Figure 7 in comparison with the JANAF values[10]. Using these vapor pressure data and free energy functions from the JANAF Tables, heats of sublimation were calculated for $C(g)$, $C_2(g)$, and $C_3(g)$ by the third law method:

$$\Delta H_{298^\circ} = T\left\{ -R\ln P + \left(\frac{F_{T^\circ} - H_{298^\circ}}{T}\right)_{solid} - \left(\frac{F_{T^\circ} - H_{298^\circ}}{T}\right)_{gas}\right\} \qquad (6)$$

these values, 173.5, 203.5, and 192.0 kcal mole^{-1} respectively, also shown in Table III, are to be compared with the best literature values listed in Table IV.

In view, however, of more recent spectroscopic work on the C_3 molecule, its heat of sublimation deserves additional attention: Gausset et al[15] have shown that the bending frequency of C_3 is around 63 - 70 cm^{-1} instead of 550 cm^{-1} on which the JANAF thermodynamic functions are based.

Table II

ION INTENSITY RATIOS $\frac{I_n}{I_1}$ FROM THE KNUDSEN-MASS SPECTROMETRIC TECHNIQUE

$T^{\circ}K$	$\frac{I_2}{I_1}$	$\frac{I_3}{I_1}$
2500	0.30	5.00
2564	0.35	5.25
2700	0.35	5.30
2703	0.40	5.33
2708	0.50	6.00
2722	0.39	4.67
2728	0.4	4.20
2745	0.43	6.22
2755	0.46	4.64
2755	0.71	6.64

15

Table III

VAPOR PRESSURES AND CALCULATED VALUES OF ΔH^{o}_{298}

OF VAPORIZATION FOR C(g), C_2(g), C_3(g)

$T^{o}K$	LOG P_{C_n} (Atm)			ΔH^{o}_{298} (kcal. mole^{-1}) for: nC(s) → Cn(g)		
	n = 1	n = 2	n = 3	n = 1	n = 2	n = 3
2564	-6.572	-7.312	-6.284	173.17	203.38	191.64
2595	-6.393	-7.132	-6.104	173.14	203.65	191.72
2562	-6.702	-7.442	-6.414	174.56	204.73	193.02
2518	-6.903	-7.642	-6.614	173.89	203.56	192.11
2565	-6.740	-7.480	-6.451	175.22	205.43	193.68
2422	-7.692	-8.431	-7.403	176.00	204.64	193.71
2452	-7.166	-7.905	-6.877	172.29	201.28	190.02
2417	-7.301	-8.040	-7.022	171.34	199.95	189.09
2515	-6.931	-7.670	-6.642	174.01	203.67	192.19
2482	-7.137	-7.876	-6.848	174.06	203.34	192.00
2700	-5.900	-6.640	-5.611	174.01	205.57	193.18

Ave.: $173.56 \pm 1, 203.5 \pm 1.1, 192.01 \pm 1.1$

16
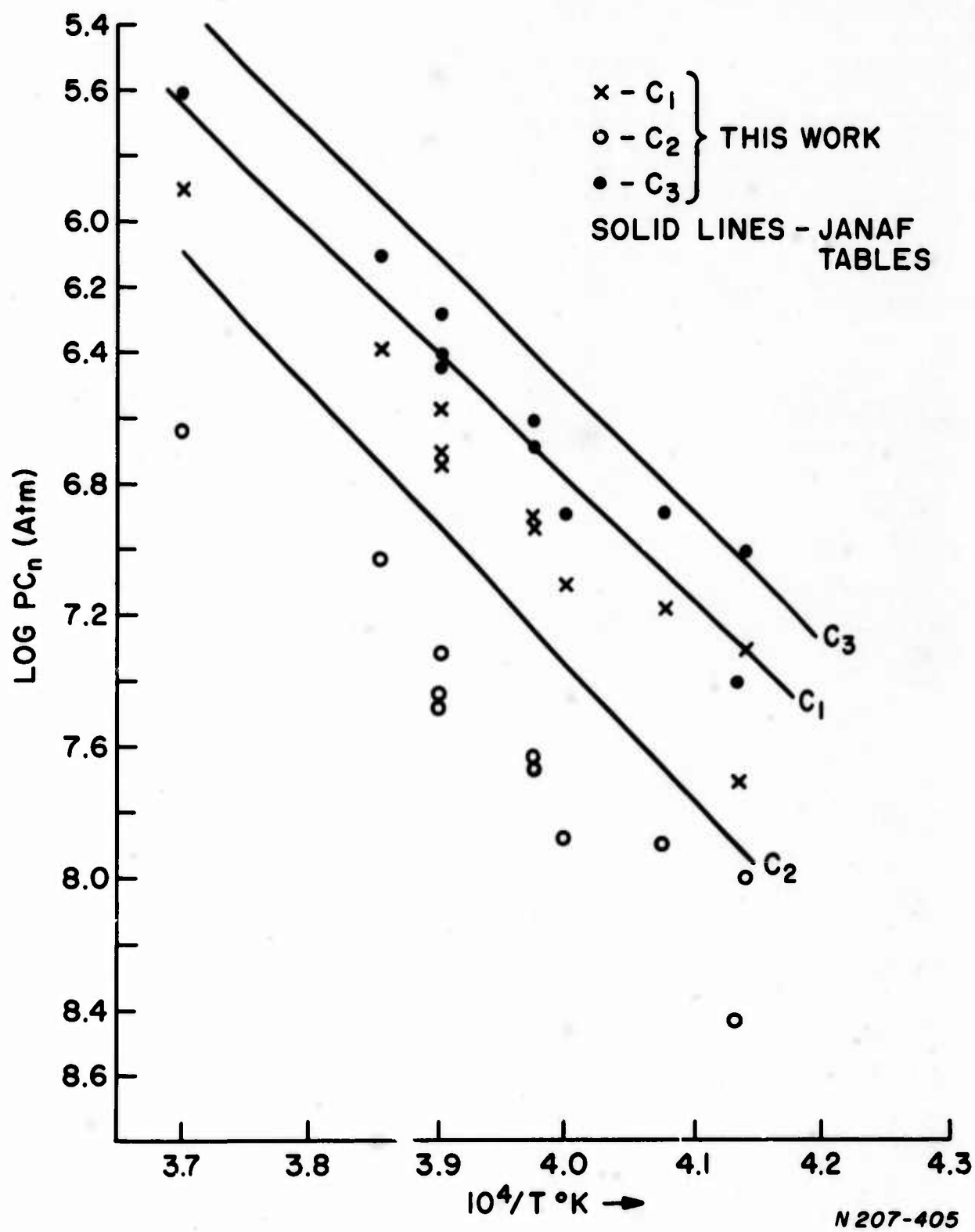
Figure 7. Vapor Pressure of Pyrolytic Graphite

17

Table IV

HEATS OF SUBLIMATION OF CARBON SPECIES

SPECIES	ΔH^o_{298} kcal mole^{-1}	REFERENCE
C_1	171.29 ($\pm$ 0.5)	Recommended by 11
	173.5 ($\pm$ 1)	This work
C_2	197.02	12
	199.02	13
	200 ($\pm$ 1.7) - (by 3rd-law)	7
	197.8 ($\pm$ 1.7) - (by 2nd-law)	7
	203.5 ($\pm$ 1)	This work
C_3	200.5	13
	190.5	14
	189.7 ($\pm$ 2.3) - (by 3rd-law)	7
	186.7 ($\pm$ 1.5) - (by 2nd-law)	7
	192.0 ($\pm$ 1.1)	This work

Free energy functions based on frequencies 63 - 70, (degenerate), 1235, and 2040 cm^{-1} made by Weltner[16] - who assumed harmonic oscilator rigid rotator - and Robiette and Strauss[17] - who took account of the considerable quartic anharmonicity of the bending vibration - are shown in Table V.

Values of $\dfrac{F^O - H^O_o}{T}$ were converted to $\dfrac{F^O - H^O_{298}}{T}$ by adding $\dfrac{H^O_o - H^O_{298}}{T}$, $H^O_o - H^O_{298} = 2.32$ kcal.

If these new values for the free energy functions are used in the third law calculation considerably higher values are obtained for the heat of vaporization:

$$\Delta H^O_{298} = 212 \text{ kcal mole}^{-1} \text{ (based on reference 16)}$$

$$\Delta H^O_{298} = 207 \text{ kcal mole}^{-1} \text{ (based on reference 17)}$$

These values depart significantly from the second law value of 186.7 ± 1.5 as reported by Drowart et al.[7] Using the higher heats and the free energy functions of Table V , vapor pressures were calculated in the temperature range 2800°K - 4600°K from equation (6) and are shown in Table VI. Figure 8 shows calculated vapor pressures based on $\Delta H^O_{298} = 207$ kcal mole^{-1} and free energy functions as calculated by Strauss.[17]

B. LANGMUIR VAPORIZATION

Since most of the vaporization phenomena of interest involve non-equilibrium conditions, it is of interest to know the vaporization coefficients for the various carbon species so that respective rates of vaporization (m) can be calculated:

$$m_i = \alpha_i P_i \left(\frac{M_i}{2\pi RT} \right)^{1/2} \qquad (7)$$

Table V

THERMODYNAMIC FUNCTIONS FOR C_3 USING A LOW BENDING

FREQUENCY (70 cm^{-1} - 63 cm^{-1})

$T^{\circ}K$	$(S^{\circ})^{(16)}$	$\dfrac{(F^{\circ}-H^{\circ}_{298})^{(16)}}{T}$	$(S^{\circ})^{(17)}$	$\dfrac{(F^{\circ}-H^{\circ}_{298})^{(17)}}{T}$
2400	84.993	73.073	82.796	71.25
2500	85.589	73.562	83.356	71.72
2600	86.162	74.036	83.895	72.18
2700	86.715	74.495	84.415	72.63
2800	87.248	74.941	84.916	73.05
3000	88.261	75.796	85.868	73.88
3200	89.210	76.605	86.760	74.66
3400	90.103	77.373	87.599	75.39
3600	90.946	78.104	88.391	76.09
3800	91.744	78.801	89.141	76.76
4000	92.502	79.467	89.854	77.40
4200	93.224	80.105	90.531	78.01
4400	93.912	80.717	91.78	78.59
4600	94.571	81.305	91/796	79.15

Table VI

CALCULATED VAPOR PRESSURES

$T^{\circ}K$	$\log P_{C_1}$	$\log P_{C_2}$	$\log P_{C_3}$ *	$\log P_{C_3}$ *
2800	-5.3565	-5.8724	-4.83	-4.771
3000	-4.4563	-4.8339	-3.795	- - - - - -
3200	-3.6713	-3.9277	-2.887	- - - - - -
3400	-2.9785	-3.129	-2.091	-1.932
3600	-2.3587	-2.422	-1.384	- - - - - -
3800	-1.804	-1.790	-0.754	-0.542
4000	-1.3191	-1.223	-0.192	- - - - - -
4200	-0.8723	-0.7105	+0.319	0.564
4400	-0.4663	-0.2455	+0.779	- - - - - -
4600	-0.0964	+0.1775	+1.196	1.466

*Based on ΔH^{o}_{298} = 207 kcal mole^{-1} and free energy functions of reference 17.

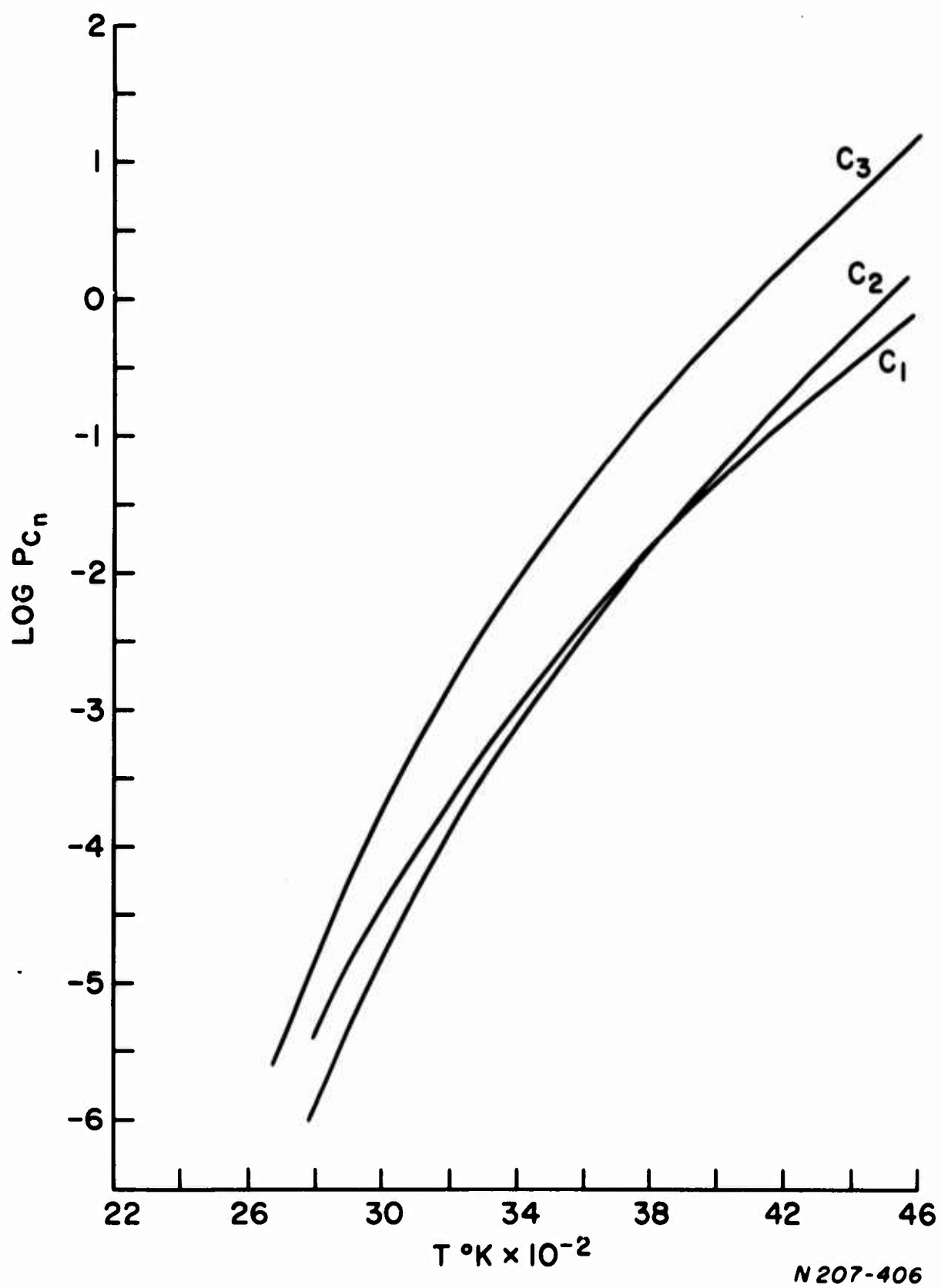**Based on ΔH^{o}_{298} = 212 kcal mole^{-1} and free energy functions of reference 16.

Figure 8. Calculated Vapor Pressures

N 207-406

22

where i = 1, 2, 3

α = vaporization coefficient

P = equilibrium vapor pressure

M = molecular weight

T = temperature in $^{\circ}$K.

By carrying out weight loss measurements in vacuum as stated before, the total rate of vaporization m was determined. This quantity can be expressed as

$$m = \sum_{i=1}^{3} a_i\, P_{C_i} \left(\frac{M_i}{2\pi\, RT}\right)^{1/2} \tag{8}$$

and is shown in Table VII and Figure 9.

By measuring relative ion intensities for the three predominant species (C, C_2, and C_3), in the mass spectrometer under both equilibrium and free vaporization conditions, I and I' respectively, ratios of vaporization coefficients can be calculated independently of any knowledge of relative cross sections and multiplier efficiencies:

For equilibrium conditions:

$$\frac{P_{C_2}}{P_{C_1}} = \frac{I_2}{I_1} \times \frac{\sigma_1}{\sigma_2} \times \frac{(E - A_1)}{(E - A_2)} \tag{9}$$

and for non-equilibrium vaporization

$$\frac{\alpha_2\, P_{C_2}}{\alpha_1\, P_{C_1}} = \frac{I'_2}{I'_1} \times \frac{\sigma_1}{\sigma_2} \frac{(E - A_1)}{(E - A_2)} \tag{10}$$

Combining equations (9) and (10)

$$\frac{\alpha_2}{\alpha_1} = \frac{I'_2}{I'_1} \times \frac{I_1}{I_2} \tag{11}$$

Similarly for

Table VII

VAPORIZATION OF PYROLYTIC GRAPHITE (FROM THE PLANE PERPENDICULAR TO THE C-AXIS) LANGMUIR-MICROBALANCE TECHNIQUE

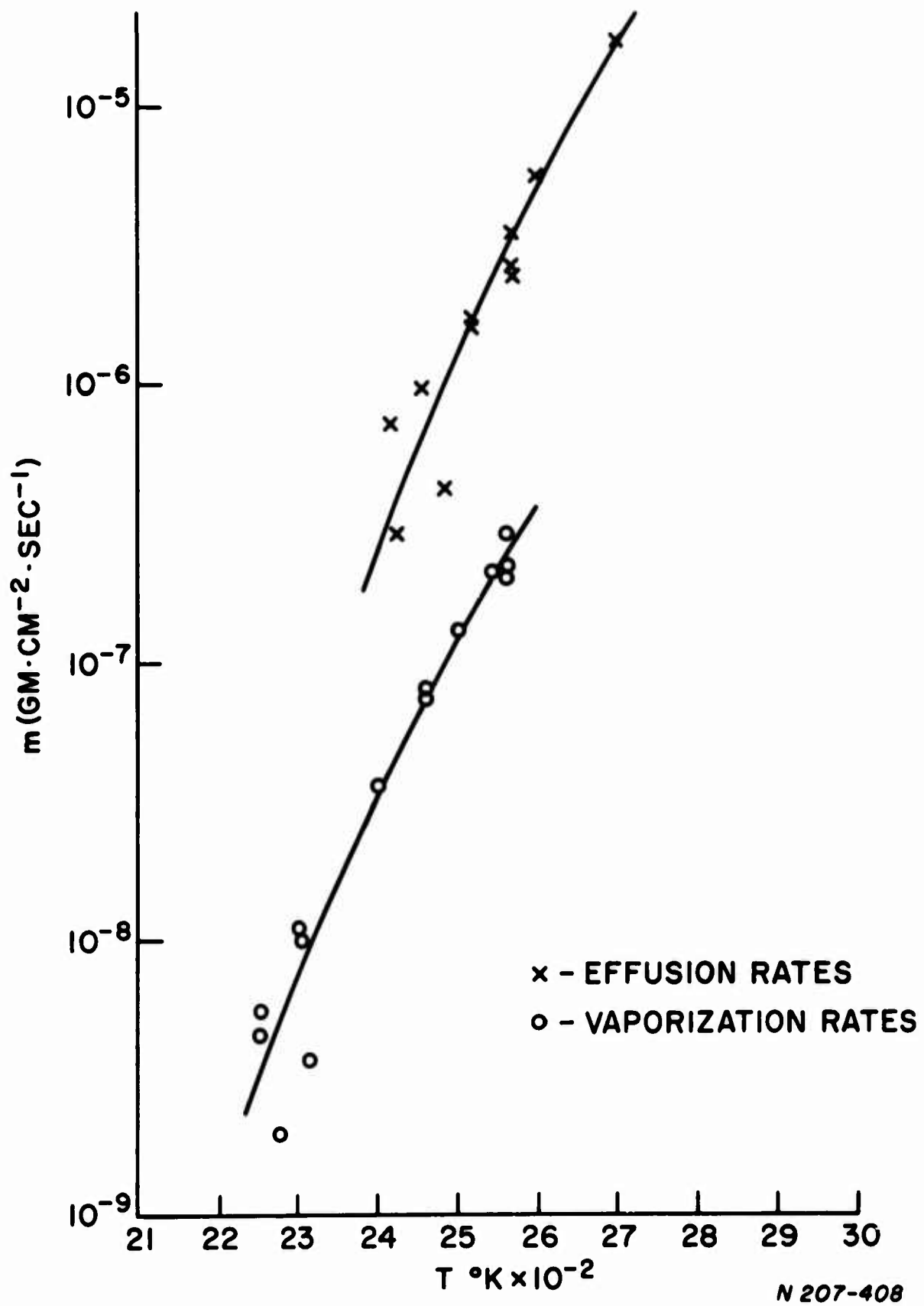| Run No.	$T^{o}K$	Rate $m_2 \times 10^{7}$ gm/cm sec
70	2460	0.80
71	2273	0.02
72	2305	0.100
73	2316	0.037
73-A	2460	0.757
78	2400	0.317
79	2540	2.145
80	2300	0.108
82	2250	0.045
83	2250	0.056
86*	2560	2.241
87*	2500	1.394
88*	2560	2.094
89*	2560	2.902

*Mechanically polished surface

Figure 9. Rates of Effusion and Vaporization for Pyrolytic Graphite

N 207-408

25

$$\frac{\alpha_1}{\alpha_3} = \frac{I'_1}{I'_3} \times \frac{I_3}{I_1} \qquad\qquad (11\text{-}A)$$

Use of equations (11), (11-A), and (8) can be made to calculate vaporization coefficients for C, C_2, and C_3.
Relative ion intensities measured in the temperature range 2618°K – 2760°K for the free vaporization from the plane perpendicular to the C-axis are shown in Figure 10 and Table VIII. Combination with data from Tables II, III, and VIII gives values for the vaporization coefficients, $\alpha_1 = 0.24$, $\alpha_2 = 0.5$, $\alpha_3 = 0.023$, also shown in Table VIII.

The over-all vaporization coefficient $\left[\dfrac{\Sigma\,\alpha_i\,P_i\sqrt{i}}{\Sigma\,P_i\,\sqrt{i}}\right]$ suggested by these measurements is 0.095 which is to be compared with the values of 10^{-3} observed by Doerhard, Goldfinger and Waelbroeck[16], 0.15 reported by Thorn and Winslow[14], and 0.07 most recently reported by Burns, Jason and Inghram[17].

The significance of the very low vaporization coefficient of C_3 is that although C_3 is the most predominant species under equilibrium conditions, this is no longer the case when equilibrium is not present. To demonstrate the significance of vaporization coefficients, calculated vaporization rates for C, C_2, and C_3 are shown in Figure 11 up to 4000°K for (a) the case of measured α's (b) for the case where α's are assumed to be unity (an assumption usually made in the absence of experimental information). It would also be interesting to make use of the non-equilibrium behavior of graphite vapor in the analyses of Scala-Vidale[20] and Scala-Gilbert[21] to determine the range where the vaporization rates (under flight conditions) are no longer controlled by an equilibrium-diffusion process. Considering the actural α's for C, C_2, and C_3, Scala and Gilbert[22] have obtained
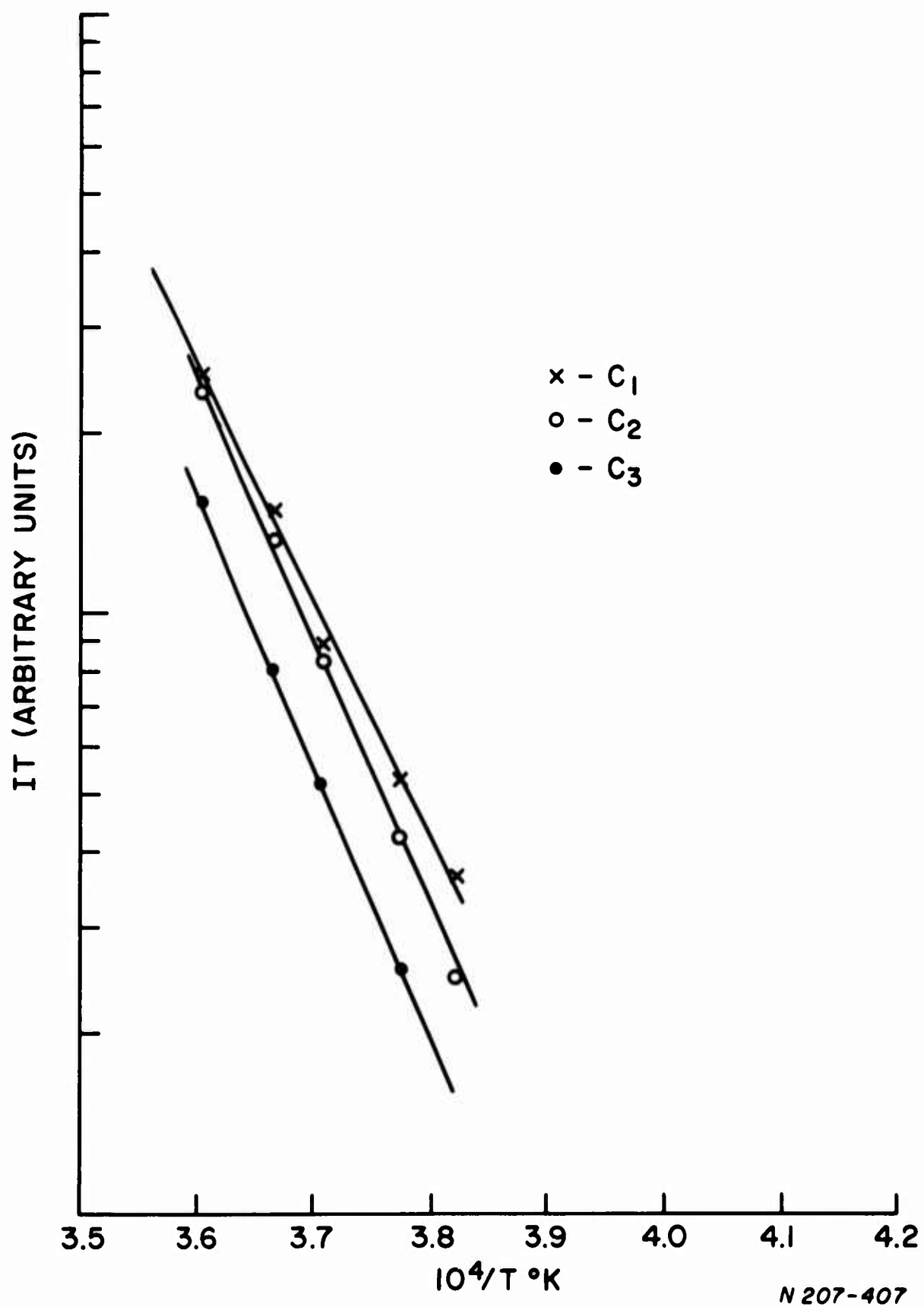
Figure 10. Langmuir Vaporization of Pyrolytic Graphite in the Mass Spectrometer

N 207-407

27

Table VIII

FREE VAPORIZATION OF PYROLYTIC GRAPHITE (FROM THE PLANE PERPENDICULAR TO THE C-AXIS)

$T^{\circ}K$	$\dfrac{I'_2}{I'_1}$	$\dfrac{I'_3}{I'_1}$	$\dfrac{\alpha_2}{\alpha_1}$	$\dfrac{\alpha_1}{\alpha_3}$
2760	0.89	0.61	1.95	9.24 ± 1.6
2740	0.91	0.56	2.1	11.11
2700	0.86	0.52	2.09 ± 0.25	10.6 ± 0.6
2660	0.80	0.48	2.28	10.93
2618	0.75	0.46	2.14	11.41
		Ave.	2.1	Ave. 10.6

$$\alpha_1 = 0.24$$
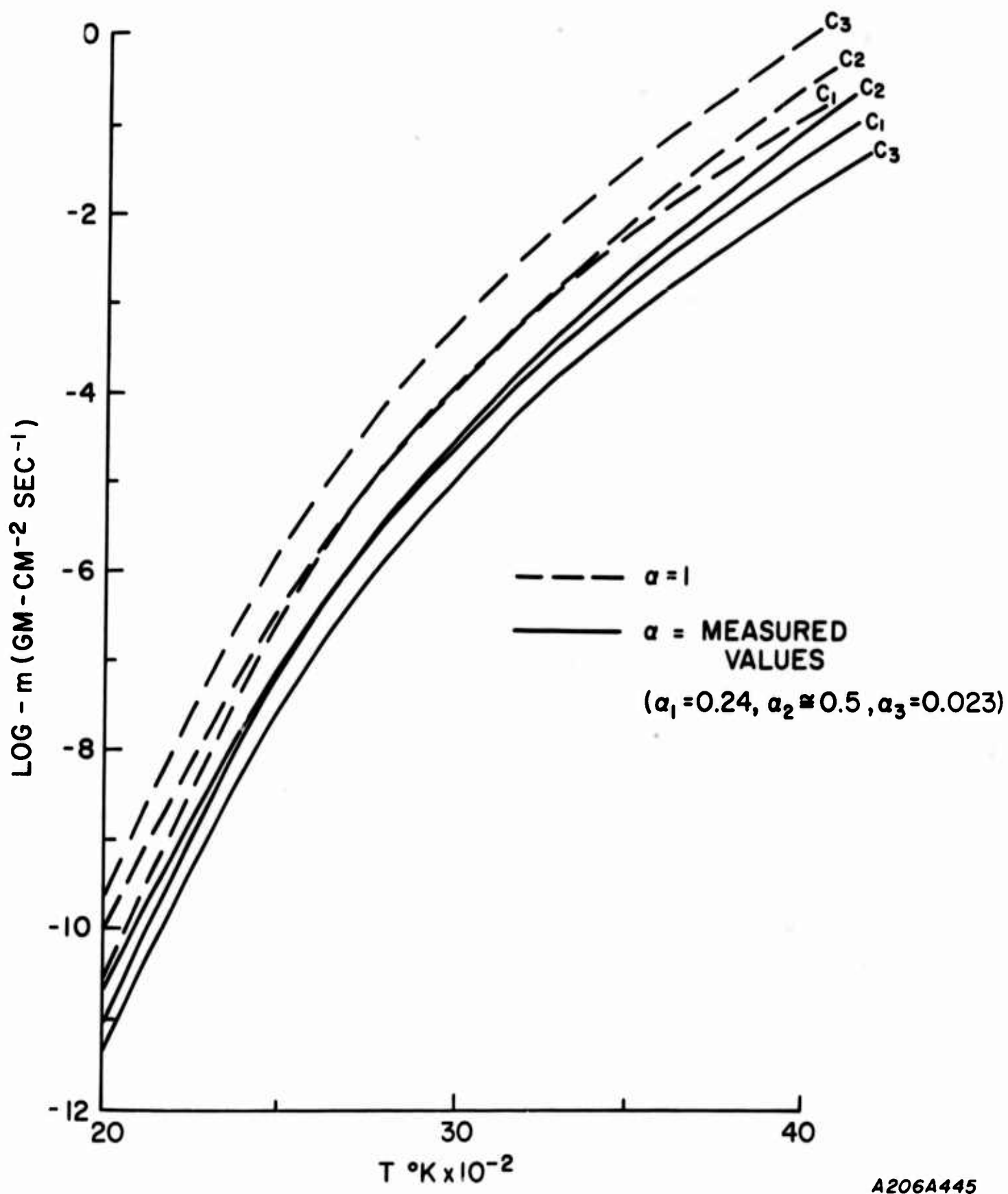
$$\alpha_2 = 0.50$$

$$\alpha_3 = 0.023$$

Figure 11.   The Effect of Vaporization Coefficients on the Composition
of the Vapor

non-equilibrium heterogeneous criteria for each species vaporizing from graphite for one hypersonic trajectory. The results indicate that the vaporization rates for C and C_2 are controlled by the equilibrium-diffusion process while the rate for C_3 is controlled by non-equilibrium vaporization.

IV. DISCUSSION AND CONCLUSIONS

This work is a rather complete study on a historically controversial subject. The attempt here was to use several complementing techniques by the same investigator and study the vaporization properties of pyrolytic graphite (which is a rather pure form of graphite). The microbalance target technique used in this study has advantages and disadvantages as previously discussed[4]. In the case of graphite vaporization the main problem is the uncertainty in the sticking coefficient of carbon vapor at the target temperature. The high reflection coefficient for C_3 measured by Chupka et al.[23], it is believed, could not have affected these microbalance results significantly since the target was kept at much lower temperatures ($< 400^{\circ}K$). Besides the conical shape of the target forces the vapor species to collide with the surface more than once, in case that the first collision did not result into condensation.

Effusion-rate and mass-spectrometric data were used to obtain vapor pressures for C, C_2, and C_3 which are essentially in agreement within less than a factor of two with the vapor pressures reported by Drowart et al.[7] based on mass spectrometric work alone. The heat of vaporization of C_3 is in some doubt in view of the conflict between the second and third-law values.

Since the same (microbalance) technique was used for the free vaporization as in the effusion studies it is expected that reflection effects are even less important in the case of vaporization coefficients; this effect would cancel out. The effect of type of graphite, surface characteristics and crystallographic plane on vaporization coefficients could very well account for the small differences in α's between this work and the work of Burns et al[19] and Thorn-Winslow[14]. The very low value of 10^{-3} reported by Doerhard et al[16] is obviously in error.

REFERENCES

1. W. S. Horton, ATL-G.E. Co. Report No. 60GL218, January 1961.

2. P. D. Zavitsanos, Semi-Annual Report for Advanced Re-entry Program. Contract No. AF 04(694)-667, June 1964.

3. P. D. Zavitsanos, TIS Report R63SD06 General Electric Company, January (1963).

4. P. D. Zavitsanos, Rev. Sci. Inst. 35, 1061 (1964).

5. P. D. Zavitsanos, J. Phys. Chem. 68, 2899 (1964).

5a. V. DeSantis, et. al. "Carbonization of Plastics and Refractory Materials", Wright Field Report, March 1965, (Contract No. AF 33(616)-6841).

6. L. Brewer, P. W. Gilles, and F. A. Jenkins, J. Chem. Phys. 16, 797 (1948).

7. J. Drowart, R. P. Burns, G. DeMaria, and M G. Inghram, J. Chem., Phys, 31, 1131 (1959).

8. W. A. Chupka and M. G. Inghram, J. Chem. Phys. 21, 371 (1953); 21 1313 (1953).

9. J. W. Otros and D. P. Stevenson, J. Chem. Phys. 78, 546 (1956).

10. JANAF, Thermochemical Tables, Dow Chemical Company, Midland, Michigan, (1961).

11. W. H. Evans, Nat. Bur. Standards Report 8504 (1964).

12. L. Brewer, W. J. Hicks, and O. H. Krikorian, J. Chem. Phys. 36, 182 (1962).

13. W. A. Chupka and M. J. Inghram, J. Phys. Chem. 59, 100 (1955).

14. R. J. Thorn and G. H. Winslow, J. Chem. Phys. 26, 186 (1957).

15. L. Gausset, G. Herzberg, A. Lagerquist, and B. Rosen, Discussions Faraday Soc. 35, 113 (1963); Astrophys. J. 142, 45, (1965).

16. W. Weltner, Jr. and D. McLeod, Jr., J. Chem. Phys. 40, 1305 (1964); Also Private Communication, Jan., 1966.

17. A. G. Robiette and H. L. Strauss, J. Chem. Phys. 44, (1966)
     Also H. L. Strauss 44, (1966). (To be published)

18. Doerhard, Goldfinger, and Waelbroeck, Bull. Soc. Chem. Beges
     62, 498 (1953).

19. R. P. Burns, A. J. Jason, and M. G. Inghram, J. Chem. Phys. 40,
     1161 (1964).

20. S. M. Scala, and G. Vidale, Intl. J. of Heat and Mass Transfer 1,
     4 (1960).

21. S. M. Scala and L. Gilbert, AIAA Journal 3, 1635 (1965).

22. Private Communication.

23. W. A. Chupka, J. Bekowitz, D. J. Meschi and H. A. Tasman,
     Advances in Mass Spectrometry, Vol. 2, p. 9, Pergamon Press
     (1963).

SPACE SCIENCES LABORATORY
MISSILE AND SPACE DIVISION

GENERAL ⬤ ELECTRIC

TECHNICAL INFORMATION SERIES

AUTHOR	SUBJECT CLASSIFICATION	NO.
P. D. Zavitsanos	Pyrolytic Graphite	R66SD31
		DATE May 1966

TITLE	G. E. CLASS
THE VAPORIZATION OF PYROLYTIC GRAPHITE	I
	GOV. CLASS None

REPRODUCIBLE COPY FILED AT MSD LIBRARY. DOCUMENTS LIBRARY UNIT. VALLEY FORGE SPACE TECHNOLOGY CENTER, KING OF PRUSSIA, PA.	NO. PAGES 34

SUMMARY   The vaporization of pyrolytic graphite was studied by the Knudsen effusion and Langmuir free vaporization techniques using a microbalance and a time-of-flight mass spectrometer.

Vapor pressures were obtained in the temperature range $2417^\circ K$ - $2700^\circ K$ for C, C_2, and C_3; respective heats of vaporization ΔH°_{298} were calculated by the third-law method.

Langmuir vaporization measurements were carried out in the temperature range $2250^\circ K$ - $2760^\circ K$. The ratios of vaporization coefficients obtained from mass spectroscopic measurements are: $\dfrac{\alpha_2}{\alpha_1} = 2.1, \dfrac{\alpha_1}{\alpha_3} = 10.6.$

Use of vapor pressure data and vaporization rates was made to arrive at an overall vaporization coefficient equal to 0.095 and individual values of $\alpha_1 = 0.24$, $\alpha_2 = 0.50$ and $\alpha_3 = 0.023$.

KEY WORDS   Vaporization, Pyrolytic Graphite

BY CUTTING OUT THIS RECTANGLE AND FOLDING ON THE CENTER LINE, THE ABOVE INFORMATION CAN BE FITTED INTO A STANDARD CARD FILE

AUTHOR _P. D. Zavitsanos_

COUNTERSIGNED _____